PCCP

PAPER

View Article Online
View Journal | View Issue

Published on 11 February 2015. Downloaded by Michigan State University on 20/01/2016 03:45:08.

Cite this: *Phys. Chem. Chem. Phys.*, 2015, **17**, 7699

A crossed molecular beam and *ab initio* study on the formation of 5- and 6-methyl-1,4-dihydronaphthalene ($C_{11}H_{12}$) *via* the reaction of *meta*-tolyl (C_7H_7) with 1,3-butadiene (C_4H_6)†

Lloyd G. Muzangwa,[a] Tao Yang,[a] Dorian S. N. Parker,[a] Ralf. I. Kaiser,*[a] Alexander M. Mebel,*[b] Adeel Jamal,[c] Mikhail Ryazantsev[d] and Keiji Morokuma*[ce]

Received 17th January 2015,
Accepted 10th February 2015

DOI: 10.1039/c5cp00311c

www.rsc.org/pccp

The crossed molecular beam reactions of the *meta*-tolyl radical with 1,3-butadiene and D6-1,3-butadiene were conducted at collision energies of 48.5 kJ mol^{-1} and 51.7 kJ mol^{-1}. The reaction dynamics propose a complex-forming reaction mechanism *via* addition of the *meta*-tolyl radical with its radical center either to the C1 or C2 carbon atom of the 1,3-butadiene reactant forming two distinct intermediates, which are connected *via* migration of the *meta*-tolyl group. Considering addition to C1 proceeds by formation of a van-der-Waals complex below the energy of the separated reactants, we propose that in cold molecular clouds holding temperatures as low as 10 K, the reaction of the *meta*-tolyl radical with 1,3-butadiene is de-facto barrier less. At elevated temperatures such as in combustion processes, the reaction can also proceed *via* addition to C2 by overcoming the entrance barrier to addition (11 kJ mol^{-1}). Eventually, the resonantly stabilized free radical intermediate $C_{11}H_{13}$ undergoes isomerization to a *cis* form, followed by rearrangement through two distinct ring closures at the *para*- and *ortho*-position of tolyl radical to yield cyclic intermediates. These intermediates then emit a hydrogen atom forming 6- and 5-methyl-1,4-dihydronaphthalene *via* tight exit transition states. The steady state branching ratio, 70.0% and 29.2%, at the collision energy of 51.7 kJ mol^{-1}, of 6- and 5-methyl-1,4-dihydronaphthalene, respectively, is determined mainly by the rates of reverse ring opening of cyclic intermediates. The formation of the thermodynamically less stable 1-*meta*-tolyl-*trans*-1,3-butadiene was found to be a less important pathway (0.8%). The reaction of the *meta*-tolyl radical with 1,3-butadiene leads without entrance barrier to two methyl substituted PAH derivatives holding 1,4-dihydronapthalene cores: 5- and 6-methyl-1,4-dihydronaphthalene thus providing a barrierless route to odd-numbered PAH derivatives under single collision conditions.

1. Introduction

Polycyclic aromatic hydrocarbons (PAHs) are ubiquitous in the Earth's environment in the form of atmospheric aerosols and soot produced as a result of incomplete combustion of fossil fuels.[1–9] PAHs have been found to be both mutagenic[10] and carcinogenic,[11] and therefore, it is clearly imperative to minimize their formation in combustion processes.[12] Kinetic models of flames are often exploited to propose likely reaction mechanisms of how PAHs and soot might be formed.[13] However, the underlying mechanisms of PAH formation and growth in hydrocarbon flames and in combustion engines are complex due to multiple simultaneous radical mediated reactions.[13,14] As a result, it is often a challenge to draw definite mechanistic conclusions from kinetic models of combustion systems.[15] PAHs are not only found in terrestrial, but also in extraterrestrial environments.[16] Here, PAH-like species such as cations, anions, and (partially) hydrogenated PAHs are thought to contribute to the unidentified infrared emission bands (UIE) and also to the diffuse interstellar bands (DIBs).[17–20] Moreover, PAHs along with their methyl-substituted counterparts have been identified in carbonaceous chondrites thus proposing extraterrestrial origins.[21–23] Also, the broad feature monitored in the UIE at 3.4 μm (2941 cm^{-1})[17–20] can be well explained by aliphatic side groups such as methyl groups.

[a] *Department of Chemistry, University of Hawaii at Manoa, Honolulu, HI 96822, USA. E-mail: ralfk@hawaii.edu*
[b] *Department of Chemistry and Biochemistry, Florida International University, Miami, FL 33199, USA*
[c] *Department of Chemistry and Cherry L. Emerson Center for Scientific Computation, Emory University, Atlanta, Georgia 30322, USA*
[d] *Biomolecular NMR Laboratory, St. Petersburg State University, Botanicheskaya 17 Staryi Peterhof, St. Petersburg, 198504, Russia*
[e] *Fukui Institute for Fundamental Chemistry, Kyoto University, Sakyo, Kyoto 606-8103, Japan. E-mail: morokuma.keiji.3a@kyoto-u.ac.jp*
† Electronic supplementary information (ESI) available. See DOI: 10.1039/c5cp00311c

Published on 11 February 2015. Downloaded by Michigan State University on 20/01/2016 03:45:08.

Despite the efforts from experimentalists and theoreticians, the underlying formation routes to PAHs are still a subject of ongoing discussion.[24] Aromatic radicals like the phenyl radical (C_6H_5) are thought to be key intermediates in PAH formation.[25] Their reactions with small, unsaturated hydrocarbons (C3 and C4) have been proposed to provide the primary link between the first aromatic ring and multiple ring species.[26–28] The formation of prototypical two ring PAHs indene (C_9H_8),[29] naphthalene ($C_{10}H_8$),[30] and 1,4-dihydronaphthalene ($C_{10}H_{10}$)[31] have recently been demonstrated to occur in reactions of the phenyl radical with allene/methylacetylene (H_2CCCH_2/CH_3CCH), vinylacetylene (CH_2CHCCH), and 1,3-butadiene ($H_2CCHCHCH_2$), respectively, under single collision conditions. The reaction leading to indene has an entrance barrier of about 14 kJ mol^{-1}, while the reactions of phenyl radicals with vinylacetylene and 1,3-butadiene involve submerged barriers implying naphthalene ($C_{10}H_8$) and 1,4-dihydro-naphthalene ($C_{10}H_{10}$) can be formed in low temperature interstellar environments, as low as 10 K, such as in molecular clouds.[30,31] On the other hand, the mechanisms to methyl substituted PAHs have not received an equal level of attention, although they appear to be produced in equal quantities in combustion environments and could be responsible for key features in the UIEs and DIBs.[21–23]

Recent studies in our group provide compelling evidence of the formation of dimethyldihydronaphthalenes *via* the reaction of the *para*-tolyl radicals ($C_6H_4CH_3$) with isoprene (C_5H_8);[15] subsequent studies also proposed a novel route to form methyl-substituted naphthalene *via* the reaction of the *para*-tolyl radicals ($C_6H_4CH_3$) with vinylacetylene (CH_2CHCCH).[32] Here, we expand these studies and apply crossed molecular beams and *ab initio* calculations to investigate the formation routes of methyl-substituted PAHs through the use of methyl-substituted aromatic radicals. Specifically, we investigate the reaction of the *meta*-tolyl radical ($C_6H_4CH_3$) with 1,3-butadiene ($H_2CCHCHCH_2$) together with its deuterated counterpart ($D_2CCDCDCD_2$) under single-collision conditions at collision energies of 48.5 and 51.7 kJ mol^{-1} respectively, leading to methyl-substituted 1,4-dihydronaphthalene isomer(s) and combine these results with electronic structure calculations to gain a full understanding of the formation of methyl substituted 1,4-dihydronapthalene isomers.

2. Experimental and theoretical methods

2.1. Experimental method and analysis

The experiments were conducted under single collision conditions by exploiting a universal crossed molecular beams machine at the University of Hawaii at Manoa.[33–37] Briefly, a helium (99.9999%; Gaspro) seeded supersonic beam of *meta*-tolyl radicals (C_7H_7) at fractions of about 0.2% was generated *via* single photon dissociation of *meta*-chlorotoluene (C_7H_7Cl, 98%, Aldrich) in the primary source chamber. This mixture was prepared by passing 1300 Torr helium gas through *meta*-chlorotoluene stored at 298 K in a stainless steel bubbler. The gas mixture was released by a piezo-electric pulse valve (Proch–Trickl) operating at 120 Hz delayed by 1882 μs after the time zero trigger; *meta*-chlorotoluene (C_7H_7Cl) was then photolyzed by focusing the 193 nm output of an Excimer laser (ComPex 110, Coherent) 1 mm downstream of the nozzle and prior to the skimmer to a spot size of 1 mm by 3 mm. The Excimer laser was operated at 60 Hz with an output of 10 mJ per pulse. A four-slot chopper wheel located after the skimmer selected a part of the *meta*-tolyl beam (C_7H_7) with a peak velocity (v_p) of 1550 ± 19 ms^{-1} and a speed ratio (S) of 9.2 ± 0.7. The second source chamber introduced a pulsed and neat 1,3-butadiene (Fluka, 99.5+%) beam (v_p = 745 ± 20 ms^{-1}; S = 8.0 ± 0.2) at a backing pressure of 550 Torr perpendicularly in the interaction region of the scattering chamber. An experiment with D6-1,3-butadiene (CDN, 99+% D) was also conducted to identify the position of the hydrogen loss, *i.e. meta*-tolyl radical *versus* 1,3-butadiene. The second pulsed valve was operated at a pulse amplitude of −400 V and an opening time of 80 μs and triggered 50 μs prior to the primary pulsed valve. This resulted in a collision energy of 48.5 ± 3.5 kJ mol^{-1} and 51.7 ± 3.5 kJ mol^{-1} with center-of-mass angles of 15.9 ± 1.3° and 17.6 ± 1.3° for the reaction between *meta*-tolyl (C_7H_7) with 1,3-butadiene (C_4H_6) and D6-1,3-butadiene (C_4D_6) beams, respectively (Table 1). The quoted velocity and speed ratio of the molecular beams are the average of about 50 measurements taken over the course of the experiment and their error boundaries are one standard deviation. Since the velocity and speed ratio are used to calculate the collision energy and center-of-mass angles the error boundaries are transferred over. Here, the maximum velocity of both primary and secondary beams is used to calculate the maximum collision energy and center-of-mass angle and *vice versa* for the minimum. The formulae used are well explained in ref. 51.

The reactively scattered products were monitored using a triply differentially pumped quadrupole mass spectrometric detector in the time-of-flight (TOF) mode after electron-impact ionization of the neutral species at an electron energy of 80 eV and an emission current of 2 mA. Time-of-flight spectra (TOF) were recorded over the full angular range of the reaction in the plane defined by the primary and the secondary reactant beams. The TOF spectra were integrated and normalized to extract the product angular distribution in the laboratory frame (LAB). To extract information on the reaction dynamics, the experimental data was transformed into the center-of-mass frame utilizing a forward–convolution routine.[38,39] This method initially assumes an angular flux distribution, $T(\theta)$, and the translational energy flux distribution, $P(E_T)$, in the center-of-mass system (CM). Laboratory TOF spectra and the laboratory angular distributions (LAB) were subsequently calculated from the $T(\theta)$ and $P(E_T)$ functions and

Table 1 Primary and secondary beam peak velocities (v_p), speed ratios (S), collision energies (E_{col}) and center-of-mass angles (Θ_{CM}) of the *meta*-tolyl (C_7H_7) radical with 1,3-butadiene

Beam	v_p (ms^{-1})	S	E_{col} (kJ mol^{-1})	Θ_{CM}
meta-Tolyl (C_7H_7)	1550 ± 19	9.2 ± 0.7	—	—
1,3-Butadiene (C_4H_6)	745 ± 20	8.0 ± 0.2	48.5 ± 3.5	15.9 ± 1.3
D6-1,3-butadiene (C_4D_6)	728 ± 20	7.9 ± 0.2	51.7 ± 3.5	17.6 ± 1.3

 This journal is © the Owner Societies 2015

Published on 11 February 2015. Downloaded by Michigan State University on 20/01/2016 03:45:08.

compared to the experimental data, the functions were iteratively adjusted until the best fit was achieved.

2.2. Computational details

Geometries of intermediates, transition states, and products involved in the reaction of the *meta*-tolyl radical with 1,3-butadiene were optimized at the hybrid density functional B3LYP level of theory with the 6-311G(d,p) basis set.[40] Vibrational frequencies and zero-point vibrational energy (ZPE) were obtained using the same B3LYP/6-311G(d,p) level of theory. Connections between different isomers and transition states have been verified by intrinsic reaction coordinate (IRC) calculations. Optimized Cartesian coordinates and computed vibrational frequencies for various species are given in the ESI.† The optimized geometries of all species were utilized in single-point calculations to refine energies at the G3(MP2,CC)//B3LYP level of theory, which is a modification[41,42] of the original Gaussian 3 (G3) scheme.[43] The final energies at 0 K were obtained using the B3LYP optimized geometries and ZPE corrections according to the following equation:

$$E_0[\mathrm{G3(MP2,CC)}] = E[\mathrm{CCSD(T)/6\text{-}311G(d,p)}] + \Delta E_{\mathrm{MP2}} + E(\mathrm{ZPE}),$$

where $\Delta E_{\mathrm{MP2}} = E[\mathrm{MP2/G3large}] - E[\mathrm{MP2/6\text{-}311G(d,p)}]$ is the basis set correction and E(ZPE) is the zero-point energy. ΔE(SO), a spin–orbit correction, and ΔE(HLC), a higher level correction, from the original G3 scheme were not included, as they are not expected to make significant contributions to relative energies. The accuracy of the G3(MP2,CC)//B3LYP/6-311G** relative energies are normally within 10 kJ mol^{-1}. The GAUSSIAN 09[44] and MOLPRO 2010[45] programs were used for the *ab initio* calculations.

RRKM theory[46–49] was used to compute energy-dependent reaction rate constants of unimolecular reaction steps following the formation of initial adducts under single-collision conditions. Available internal energy for each species, including intermediates and transition states, was taken as the energy of chemical activation plus the collision energy assuming the latter is dominantly converted into the internal vibrational energy. Harmonic approximation was used for calculations of the density and number of states required to compute the rate constants. Phenomenological first-order rate equations were then solved within the steady-state approximation using the RRKM rate constants to evaluate product branching ratios for decomposition of various initial reaction adducts formed by the addition of *meta*-tolyl radical to 1,3-butadiene.

3. Experimental results

3.1. Laboratory data

In the reaction of the *meta*-tolyl radical (C_7H_7; 91 u) with 1,3-butadiene (C_4H_6; 54 u), reactive scattering signal was monitored at mass-to-charge ratios from m/z 144 ($C_{11}H_{12}^+$) down to m/z 142 ($C_{11}H_{10}^+$). At each angle, the TOF spectra recorded at lower m/z ratios of 143 ($C_{11}H_{11}^+$) and 142 ($C_{11}H_{12}^+$) depicted identical profiles, after scaling, compared to those at m/z 144 and could be fit with identical center-of-mass functions as

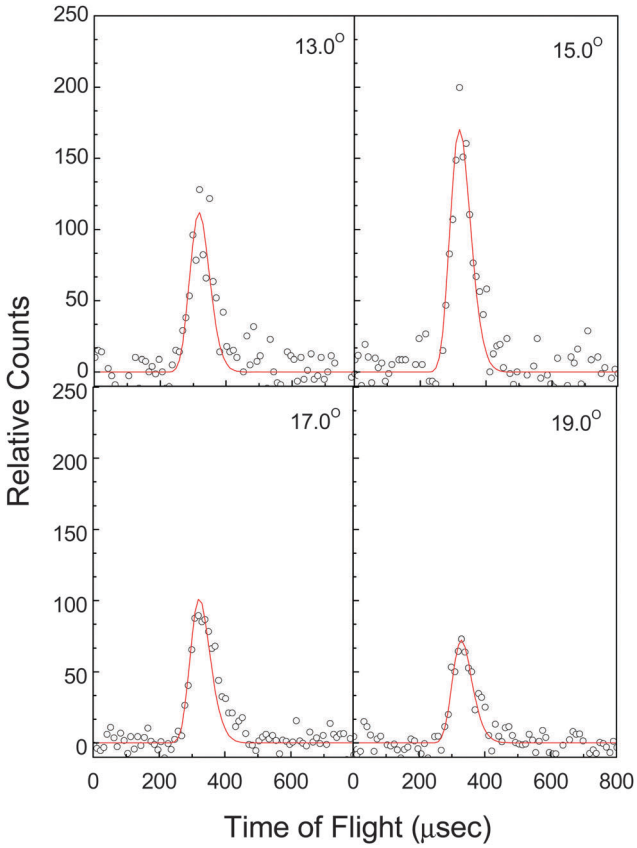

Fig. 1 Time-of-flight data at various laboratory angles for the reaction of the *meta*-tolyl (C_7H_7) with 1,3-butadiene (C_4H_6) recorded at m/z 144 ($C_{11}H_{12}^+$) at a collision energy of 48.5 ± 3.5 kJ mol^{-1}. The circles represent the experimental data and the red lines the fits.

those data taken at m/z 144. This indicated that signal at m/z 143 results from dissociative ionization of the parent molecule ($C_{11}H_{12}$) in the electron impact ionizer of the detector. Further, we can determine that only the *meta*-tolyl radical *versus* hydrogen atom exchange pathway is open within this mass range. Accounting for the signal-to-noise ratio and data accumulation time, we recorded the TOF spectra at the strongest signal ion at m/z 144 (Fig. 1). We also probed the potential formation of an adduct at m/z 145 ($C_{11}H_{13}^+$); however, once again, the TOFs at m/z 145 and 144 overlapped, after scaling, indicating that ion counts at m/z 145 originate from the naturally occurring ^{13}C-labelled product $^{13}CC_{10}H_{12}$, which is formed at a level of about 12% compared to the $C_{11}H_{12}$ product. The collected TOF spectra at m/z 144 can be exploited to derive the laboratory angular distribution of signal recorded at m/z 144 ($C_{11}H_{12}^+$) by integrating the TOF spectra at each angle and accounting for the data accumulation time (Fig. 2). Here, the LAB distribution is nearly forward–backward symmetric in the laboratory frame and also relatively narrowly spread only over about 20° in the scattering plane defined by both the *meta*-tolyl and the 1,3-butadiene supersonic beams. These findings propose indirect scattering dynamics *via* formation of a $C_{11}H_{13}$ complex. Note that reactive signal from a methyl (CH_3) loss channel, which would yield ($C_{10}H_{10}$) products at

Published on 11 February 2015. Downloaded by Michigan State University on 20/01/2016 03:45:08.

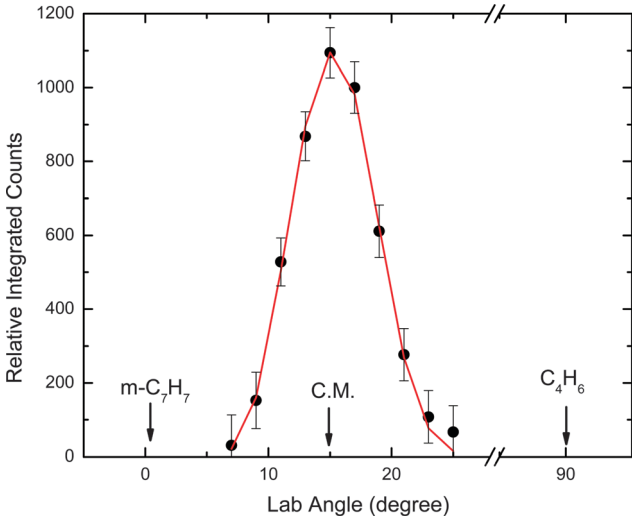

Fig. 2 Laboratory angular distribution of the $C_{11}H_{12}$ reaction product formed in the reaction of *meta*-tolyl (C_7H_7) plus 1,3-butadiene (C_4H_6) recorded at *m*/*z* 144 ($C_{11}H_{12}^+$) at collision energy of 48.5 ± 3.5 kJ mol^{-1}. The circles present the experimental data, and the red line represents the fits utilizing the best fit center-of-mass functions. C.M. designates the center-of-mass angle. The error bars are derived as the standard deviation from the result of 5 angular scans.

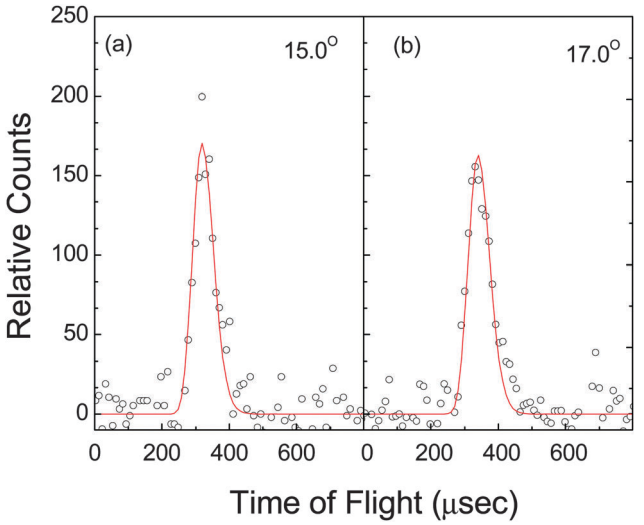

Fig. 3 Time-of-flight data recorded at the center-of-mass for the atomic hydrogen loss pathway in the reaction of *meta*-tolyl (C_7H_7) with 1,3-butadiene (C_4H_6) recorded at *m*/*z* 144 ($C_{11}H_{12}^+$) (a) and D6-1,3-butadiene (C_4D_6) recorded at *m*/*z* 150 ($C_{11}H_6D_6^+$) (b), respectively. The circles present the experimental data and the red lines present the fits utilizing the best fit center-of-mass functions.

m/*z* 130, was searched for. However, no reactive scattering signal was observed, and we conclude the methyl loss pathway is closed.

Having established the presence of the *meta*-tolyl *versus* atomic hydrogen exchange and the formation of $C_{11}H_{12}$ isomers (Fig. 1 and 2), we are attempting now to elucidate the position of the atomic hydrogen loss, *i.e.* a hydrogen loss from the *meta*-tolyl radical and/or from the 1,3-butadiene reactant. To answer this question, we conducted the reaction of the *meta*-tolyl radical (C_7H_7; 91 u) with deuterated 1,3-butadiene (C_4D_6; 60 u) and probed the scattering signal at the center-of-mass reference angle.

$$C_7H_7 + 1,3\text{-}C_4D_6 \rightarrow \begin{cases} C_{11}H_7D_5\,(m/z = 149) + D \\ C_{11}H_6D_6\,(m/z = 150) + H \end{cases} \quad (1)$$

If a hydrogen atom elimination takes place from the *meta* tolyl group, reactive scattering signal should be observable for the atomic hydrogen loss at *m*/*z* 150 ($C_{11}H_6D_6^+$); if an atomic deuterium loss pathway is present from the D6-1,3-butadiene reactant, we should yield signal at *m*/*z* 149 ($C_{11}H_7D_5^+$). Here, we observed reactive scattering signal at *m*/*z* 151, 150, and 149; the intensity of signal at *m*/*z* 151 suggests that the latter originates from ^{13}C substituted $C_{11}H_6D_6$, *i.e.* $^{13}CC_{10}H_6D_6$, which occurs at a level of about 12%. Signal at *m*/*z* 150 was significantly stronger than the other masses and explicitly indicates the existence of an atomic hydrogen elimination from the *meta*-tolyl radical. Signal at *m*/*z* 149 was weak and could originate from dissociative electron impact ionization of the $C_{11}H_6D_6$ product ($C_{11}H_5D_6^+$) and/or from an atomic deuterium loss ($C_{11}H_7D_5^+$). Considering that within our error limits, the intensity of reactive scattering signal at *m*/*z* 144 ($C_{11}H_{12}^+$) (*m*-tolyl/1,3-butadiene) is equal to signal at *m*/*z* 150 ($C_{11}H_6D_6^+$) (Fig. 3) within 15%, we conclude that that the atomic hydrogen elimination channel from the *m*-tolyl radical represents the dominant route.

3.2. Center of mass translational energy, $P(E_T)$, and angular distribution, $T(\theta)$

The laboratory data verify the formation of $C_{11}H_{12}$ isomers plus a hydrogen atom loss originating from the *meta*-tolyl radical in the reaction between the *meta*-tolyl radical with 1,3-butadiene. We are converting now the laboratory data into the center-of-mass reference frame and discuss the center-of-mass angular $T(\theta)$ and translational energy $P(E_T)$ distributions. Most importantly, the TOF data (Fig. 1) and LAB distribution (Fig. 2) could be fit with only one reaction channel originating from the *meta*-tolyl radical (77 u) plus 1,3-butadiene (54 u) shown as the red line in Fig. 1 and 2. The corresponding center-of-mass translational energy distribution, $P(E_T)$, is depicted in Fig. 4. This fit could be obtained with a distribution extending to a maximum translational energy release, E_{Tmax}, of 170 ± 30 kJ mol^{-1} at a collision energy of 48.5 ± 3.5 kJ mol^{-1}. For those molecules born without internal excitation, the high-energy cutoff represents the sum of the absolute energy of the reaction plus the collision energy; this allows us to determine the reaction to be exoergic by 121 ± 34 kJ mol^{-1}. These data correlate nicely with the computed exoergicities to form the 5-methyl-1,4-dihydronaphthalene and 6-methyl-1,4-dihydronaphthalene isomers of 97 kJ mol^{-1} and 98 kJ mol^{-1}, respectively. Finally, we determined the fraction of available energy channeled into the translational degrees of freedom of the products to be about 35 ± 5% of the total available energy. This order of magnitude indicates indirect scattering dynamics.[50] In addition, the center-of-mass translation energy distribution shows a pronounced distribution maximum in the range of 25–50 kJ mol^{-1}, *i.e.* a peaking well away from zero translational energy. This finding

 This journal is © the Owner Societies 2015

Published on 11 February 2015. Downloaded by Michigan State University on 20/01/2016 03:45:08.

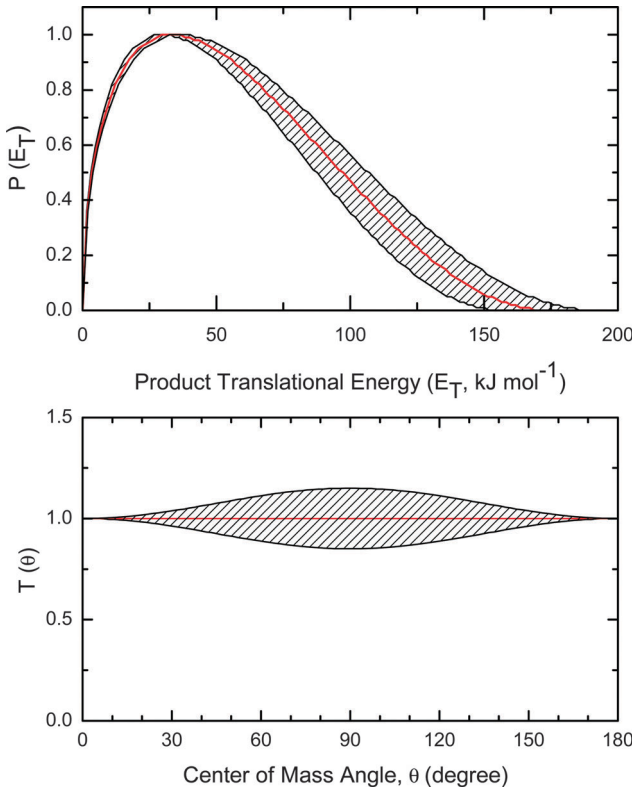

Fig. 4 Center-of-mass translational energy distribution (top) and angular distribution (bottom) for the reaction of *meta*-tolyl (C_7H_7) with 1,3-butadiene (C_4H_6) to form ($C_{11}H_{12}$) plus atomic hydrogen. The hatched area represents the possible fits that remain within the error boundaries of the LAB angular distribution shown in Fig. 2.

likely indicates a tight exit transition state when the $C_{11}H_{13}$ intermediate(s) dissociates to the final products. According to the principle of microscopic reversibility of a chemical reaction, the reverse reaction of hydrogen atom addition to the $C_{11}H_{12}$ isomer is therefore expected to have an entrance barrier.[51]

The center-of-mass angular distribution helps us to gain additional ESI† on the reaction dynamics. Here, the angular flux distribution shows intensity over the complete angular range from 0° to 180° (Fig. 4) and also a forward–backward symmetry. This finding indicates that the reaction follows indirect scattering dynamics *via* complex ($C_{11}H_{13}$) formation. The forward–backward symmetry proposes that the lifetime(s) of the $C_{11}H_{13}$ intermediate(s) is longer its rotational period. The poorly polarized $T(\theta)$ is indicative of an insignificant coupling between the initial (L) and final (L') orbital angular momentum of the reaction system.[51] This inefficient coupling is attributed to the lightness of the ejected hydrogen atom that is not able to carry away significant angular momentum when emitted from the decomposing $C_{11}H_{13}$ complex.

4. Discussion

4.1. Product isomer identification

From the laboratory data alone, we can verify the formation of $C_{11}H_{12}$ isomer(s) plus atomic hydrogen. We are now considering the energetics of the reaction and attempt to identify the product isomer by comparing the experimentally determined reaction energy of 121 ± 34 kJ mol^{-1} with theoretically calculated energies for distinct $C_{11}H_{12}$ isomers. Note that we considered a broad variety of reaction channels analogous to those studied earlier for the reaction of the phenyl radical with 1,3-butadiene,[31] but in this discussion we concentrate only on the most important channels (Fig. 5), relevant to our experimental observations. Here, the experimentally determined reaction exoergicity correlates reasonably well with the theoretically predicted data for the formation of 5-methyl-1,4-dihydronaphthalene and 6-methyl-1,4-dihydronaphthalene isomers of 97 kJ mol^{-1} and 98 kJ mol^{-1}, respectively. The formation of a third isomer – the monocyclic 1-*meta*-tolyl-*trans*-1,3-butadiene – is associated with a reaction energy of −36 kJ mol^{-1}; this is 85 kJ mol^{-1} higher in energy than observed experimentally. Therefore, based on the energetics alone, we can conclude that at least the thermodynamically more stable 5- and/or 6-methyl-1,4-dihydronaphthalene isomer(s) are formed.

4.2. Proposed reaction dynamics

Before we unravel the underlying reaction dynamics, we would like to compile the key results obtained.

R1: in the *meta*-tolyl–1,3-butadiene system, the experimental data suggest the formation of $C_{11}H_{12}$ isomer(s) *via* hydrogen atom elimination involving indirect scattering dynamics through long-lived $C_{11}H_{13}$ intermediate(s) and tight exit transition state(s). A comparison of the experimentally determined reaction energy with the theoretically obtained ones suggests at least the formation of the 5- and/or 6-methyl-1,4-dihydronaphthalene isomer(s) with potentially less important contributions from the 1-*meta*-tolyl-*trans*-1,3-butadiene isomer.

R2: in the *meta*-tolyl–D6-1,3-butadiene system, the experimental data suggest an atomic hydrogen loss from the *meta*-tolyl group. The intensity of this channel is about 85% of the intensity for *meta*-tolyl–1,3-butadiene system suggesting that the dominant reactive scattering signal originates from a hydrogen loss from the *meta*-tolyl reactant (85%) with potentially minor contributions (15%) from the 1,3-butadiene reactant.

We now turn our attention to the reaction mechanism proposed by the calculated potential energy surface as shown in Fig. 5 (bottom). According to the calculations, the reaction of the *meta*-tolyl radical with 1,3-butadiene occurs without a barrier to produce initially a weakly-bound (6 kJ mol^{-1}) van-der-Waals complex [0]. The latter isomerizes *via* a barrier of only 4 kJ mol^{-1} through addition of the *meta*-tolyl radical with its radical center to the C1 carbon atom of the 1,3-butadiene reactant yielding a doublet radical intermediate [1], which is resonantly stabilized. The barrier to addition lies below the energy of the separated reactants and hence can be classified as a submerged barrier. Note that the resonantly stabilized free radical (RSFR) intermediate [1] can also be formed *via* addition of the *meta*-tolyl radical to the C2 carbon atom of 1,3-butadiene forming [5], which then isomerizes *via meta*-tolyl group migration to [1]. However, the initial addition to C2 is associated with an entrance barrier of 11 kJ mol^{-1}. Intermediate [1] – either

Published on 11 February 2015. Downloaded by Michigan State University on 20/01/2016 03:45:08.

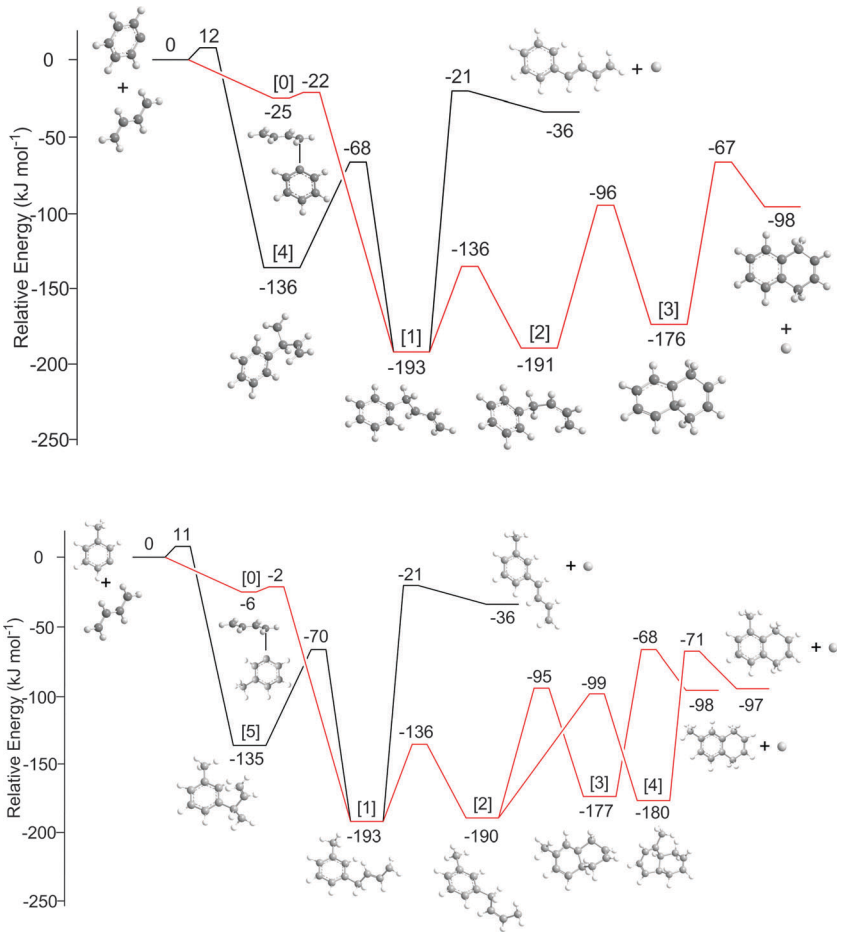

Fig. 5 Potential energy surface for the reaction of the *meta*-tolyl radical with 1,3-butadiene (bottom) in comparison to the potential energy surface of the phenyl-1,3-butadiene reaction (top). Energies for intermediates, transition states, and products are given relative to the reactants energy (in kJ mol^{-1}) at the at the G3(MP2,CC)//B3LYP/6-311G** level of theory.

formed *via* initial addition to C1 or C2 – can either lose a hydrogen atom forming the 1-*meta*-tolyl-*trans*-1,3-butadiene isomer *via* a transition state located only 15 kJ mol^{-1} above the energy of the separated products. Alternatively, the *trans* intermediate [1] undergoes an isomerization to a cis intermediate [2] involving a low barrier of 57 kJ mol^{-1}. Based on the non-symmetric *meta*-tolyl reactant (C_s symmetry), ring closure of [2] can either proceed *via* formation of a carbon–carbon bond to the *para*- or *ortho*-positions of the tolyl radical to give cyclic intermediates [3] and [4], respectively. Both intermediates can undergo unimolecular decomposition *via* atomic hydrogen loss from the *para* or *ortho* position with respect to the methyl group of the tolyl moiety, forming 6- and 5-methyl-1,4-dihydronaphthalene in overall exoergic reactions (−98 and −97 kJ mol^{-1}) *via* tight transition states. Based on our statistical (RRKM) rate calculations[46–49] and a steady-state approximation, we predict branching ratios at collision energy of 51.7 kJ mol^{-1} to be 70.0% to 29.2% to 0.8% for 6-methyl-1,4-dihydronaphthalene to 5-methyl-1,4-dihydronaphthalene to 1-*meta*-tolyl-*trans*-1,3-butadiene, respectively. The steady state branching ratio between 6-methyl-1,4-dihydro-naphthalene to 5-methyl-1,4-dihydronaphthalene is determined mainly by the rates of the reversed ring opening reaction of cyclic intermediates [3] and [4]. With the lower reversed barrier of [4] → [2] relative to [3] → [2] and the higher density of states for [3] as compared to [4] due to a looser structure of [3], where the methyl group is located far from the extra hydrogen atom, [4] has a lower concentration than [3] and thus lower branching to 6-methyl-1,4-dihydronaphthalene.

The computationally predicted reaction mechanism is fully supported by our experimental findings. First, the comparison of the experimentally determined reaction energy with the theoretically obtained data supports the predominant formation of the 5- and/or 6-methyl-1,4-dihydronaphthalene isomer(s) (85%). This correlates with the computed fraction of 99% forming the thermodynamically most stable isomers. Secondly, the experimentally observed tight exit transition state of 25–50 kJ mol^{-1} is also reproduced well by the calculations to be 26 kJ mol^{-1} and 30 kJ mol^{-1} forming 5- and 6-methyl-1,4-dihydronaphthalene, respectively. Thirdly, the predicted reaction mechanism and the experimental findings both indicate that the dominant hydrogen loss channel originates from the *meta*-tolyl moiety forming the 5- and/or 6-methyl-1,4-dihydronaphthalene isomers. Fourthly, the reaction mechanism follows indirect scattering dynamics through long-lived $C_{11}H_{13}$ intermediate(s).

 This journal is © the Owner Societies 2015

Published on 11 February 2015. Downloaded by Michigan State University on 20/01/2016 03:45:08.

A comparison of the title reaction with the related reaction of the phenyl radical with 1,3-butadiene forming 1,4-dihydronaphthalene studied earlier in our group both experimentally and computationally (Fig. 5) suggests that the methyl group acts as a spectator and is not actively engaged in the chemistry of the *meta*-tolyl plus 1,3-butadiene reaction. Here, the replacement of the hydrogen atom by the methyl group only changes the energetics of the intermediates and transition states by 1–2 kJ mol^{-1}. Further, the effect on the overall reaction energies is minor (98 kJ mol^{-1} *versus* 98 kJ mol^{-1}/97 kJ mol^{-1}). However, considering the asymmetry of the *meta*-tolyl radical reactant, intermediate [2] can undergo ring closure *via* two distinct pathways by forming a carbon–carbon bond either to the *ortho* or *para* position with respect to the methyl group. The production of 6-methyl-1,4-dihydronaphthalene is preferred to 5-methyl-1,4-dihydronaphthalene.

5. Conclusions

We have conducted crossed molecular beam studies of the reactions of the *meta*-tolyl radical with 1,3-butadiene and D6-1,3-butadiene at a collision energies of 48.5 kJ mol^{-1} and 51.7 kJ mol^{-1} respectively. The reaction chemical dynamics propose a complex-forming reaction mechanism *via* eventual addition of the *meta*-tolyl radical with its radical center either to the C1 or C2 carbon atom forming two distinct intermediates, which are connected *via* migration of the *meta*-tolyl group. Considering that the formation of a van-der-Waals complex [0] precedes the addition to C1, we can propose that in cold molecular clouds holding temperatures as low as 10 K, the reaction of the *meta*-tolyl radical with 1,3-butadiene is de-facto barrier less and proceeds solely *via* van-der-Waals complex followed by isomerization through addition of the radical to C1. However, at elevated temperatures such as in combustion processes, the reaction can also proceed *via* addition to C2 by overcoming the entrance barrier to addition. Eventually, the resonantly stabilized free radical intermediate $C_{11}H_{13}$ undergoes rearrangements involving *trans–cis* isomerization and two distinct ring closures forming eventually 5- and 6-methyl-1,4-dihydronaphthalene *via* tight transition states in exoergic reactions (97 kJ mol^{-1} and 98 kJ mol^{-1}) (85%) The formation of the thermodynamically less stable 1-*meta*-tolyl-*trans*-1,3-butadiene was found to be only a less important pathway (15%). In conclusion, we demonstrated that the reaction of the *meta*-tolyl radical with 1,3-butadiene can lead without entrance barrier to two methyl substituted PAH derivatives holding 1,4-dihydronapthalene cores: 5- and 6-methyl-1,4-dihydronaphthalene thus providing a barrierless route to odd-numbered PAH derivatives under single collision conditions.

Acknowledgements

This material is based upon work supported by the U.S. DOE Office of Science, Office of Basic Energy Sciences (DE-FG02-03ER15411 to University of Hawaii and DE-FG02-04ER15570 to FIU) and also by the Air Force Office of Scientific Research (FA9550-12-1-0472) at Emory University. A.M.M. would like to acknowledge the Instructional & Research Computing Center (IRCC, web: http://ircc.fiu.edu) at Florida International University for providing HPC computing resources that have contributed to the research results reported within this paper.

References

1 C. Venkataraman and S. K. Friedlander, *Environ. Sci. Technol.*, 1994, **28**, 563–572.
2 J. O. Allen, N. M. Dookeran, K. A. Smith, A. F. Sarofim, K. Taghizadeh and A. L. Lafleur, *Environ. Sci. Technol.*, 1996, **30**, 1023–1031.
3 F. P. Perera, *Science*, 1997, **278**, 1068–1073.
4 A. M. Mebel, V. V. Kislov and R. I. Kaiser, *J. Am. Chem. Soc.*, 2008, **130**, 13618–13629.
5 Z. Tian, W. J. Pitz, R. Fournet, P. A. Glaude and F. Battin-Leclerc, *Proc. Combust. Inst.*, 2011, **33**, 233–241.
6 B. Yang, Y. Li, L. Wei, C. Huang, J. Wang, Z. Tian, R. Yang, L. Sheng, Y. Zhang and F. Qi, *Proc. Combust. Inst.*, 2007, **31**, 555–563.
7 Y. Li, L. Zhang, Z. Tian, T. Yuan, J. Wang, B. Yang and F. Qi, *Energy Fuels*, 2009, **23**, 1473–1485.
8 C. Huang, L. Wei, B. Yang, J. Wang, Y. Li, L. Sheng, Y. Zhang and F. Qi, *Energy Fuels*, 2006, **20**, 1505–1513.
9 N. Olten and S. M. Senkan, *Combust. Flame*, 1999, **118**, 500–507.
10 B. J. Finlayson-Pitts and J. N. Pitts, Jr., *Science*, 1997, **276**, 1045–1052.
11 W. M. Baird, L. A. Hooven and B. Mahadevan, *Environ. Mol. Mutagen.*, 2005, **45**, 106–114.
12 X. B. Gu, F. T. Zhang and R. I. Kaiser, *J. Phys. Chem. A*, 2009, **113**, 998–1006.
13 M. Frenklach, *Phys. Chem. Chem. Phys.*, 2002, **4**, 2028–2037.
14 N. W. Moriarty, W. A. Lester and M. Frenklach, *Abstr. Pap. Am. Chem. Soc.*, 2002, **224**, U580.
15 B. B. Dangi, T. Yang, R. I. Kaiser and A. M. Mebel, *Phys. Chem. Chem. Phys.*, 2014, **16**, 16805–16814.
16 *The Universe as Seen by ISO, ESA, SP-427*, ed. P. Cox and M. F. Kessler, Europen Space Agency, The Netherlands, 1999.
17 S. Kwok and Y. Zhang, *Nature*, 2011, **479**, 80–83.
18 A. Li and B. T. Draine, *Astrophys. J.*, 2012, **760**, L31–L35.
19 T. B. Geballe, A. G. G. M. Tielens, S. Kwok and B. J. Hrivnak, *Astrophys. J.*, 1992, **387**, L89–L91.
20 B. J. Hrivnak, T. B. Geballe and S. Kwok, *Astrophys. J.*, 2007, **662**, 1059–1066.
21 J. E. Elsila, N. P. De Leon, P. R. Buseck and R. N. Zare, *Geochim. Cosmochim. Acta*, 2005, **69**, 1349–1357.
22 M. K. Spencer, M. R. Hammond and R. N. Zare, *Proc. Natl. Acad. Sci. U. S. A.*, 2008, **105**, 18096–18101.
23 M. A. Sephton, *Nat. Prod. Rep.*, 2002, **19**, 292–311.
24 X. B. Gu, F. T. Zhang, R. I. Kaiser, V. V. Kislov and A. M. Mebel, *Chem. Phys. Lett.*, 2009, **474**, 51–56.
25 R. S. Tranter, S. J. Klippenstein, L. B. Harding, B. R. Giri, X. Yang and J. H. Kiefer, *J. Phys. Chem. A*, 2010, **114**, 8240–8261.

Published on 11 February 2015. Downloaded by Michigan State University on 20/01/2016 03:45:08.

26 B. Shukla, A. Susa, A. Miyoshi and M. Koshi, *J. Phys. Chem. A*, 2008, **112**, 2362–2369.
27 B. Shukla, A. Susa, A. Miyoshi and M. Koshi, *J. Phys. Chem. A*, 2007, **111**, 8308–8324.
28 H. Richter, T. G. Benish, O. A. Mazyar, W. H. Green and J. B. Howard, *Proc. Combust. Inst.*, 2000, **28**, 2609–2618.
29 D. S. N. Parker, F. Zhang, R. I. Kaiser, V. V. Kislov and A. M. Mebel, *Chem. – Asian J.*, 2011, **6**, 3035.
30 D. S. N. Parker, F. Zhang, Y. S. Kim, R. I. Kaiser, A. Landera, V. V. Kislov, A. M. Mebel and A. G. G. M. Tielens, *Proc. Natl. Acad. Sci. U. S. A.*, 2012, **109**, 53–58.
31 R. I. Kaiser, D. S. N. Parker, F. Zhang, A. Landera, V. V. Kislov and A. M. Mebel, *J. Phys. Chem. A*, 2012, **116**, 4248–4258.
32 D. S. N. Parker, B. B. Dangi, R. I. Kaiser, A. Jamal, M. N. Ryazantsev, K. Morokuma, A. Korte and W. Sander, *J. Phys. Chem. A*, 2014, **118**, 2709–2718.
33 F. T. Zhang, S. Kim and R. I. Kaiser, *Phys. Chem. Chem. Phys.*, 2009, **11**, 4707–4714.
34 Y. Guo, X. B. Gu, E. Kawamura and R. I. Kaiser, *Rev. Sci. Instrum.*, 2006, 77.
35 X. B. Gu, Y. Guo, E. Kawamura and R. I. Kaiser, *J. Vac. Sci. Technol., A*, 2006, **24**, 505–511.
36 R. I. Kaiser, P. Maksyutenko, C. Ennis, F. Zhang, X. Gu, S. P. Krishtal, A. M. Mebel, O. Kostko and M. Ahmed, *Faraday Discuss.*, 2010, **147**, 429–478.
37 X. B. Gu, Y. Guo, F. T. Zhang, A. M. Mebel and R. I. Kaiser, *Faraday Discuss.*, 2006, **133**, 245–275.
38 M. Vernon, PhD thesis, University of California, Berkeley, 1981.
39 M. S. Weiss, PhD thesis, University Of California, Berkeley, 1986.
40 P. J. Stephens, F. J. Devlin, C. F. Chabalowski and M. J. Frisch, *J. Phys. Chem.*, 1994, **98**, 11623–11627.
41 A. G. Baboul, L. A. Curtiss, P. C. Redfern and K. Raghavachari, *J. Chem. Phys.*, 1999, **110**, 7650–7657.
42 L. A. Curtiss, K. Raghavachari, P. C. Redfern, A. G. Baboul and J. A. Pople, *Chem. Phys. Lett.*, 1999, **314**, 101–107.
43 L. A. Curtiss, K. Raghavachari, P. C. Redfern, V. Rassolov and J. A. Pople, *J. Chem. Phys.*, 1998, **109**, 7764–7776.
44 M. J. Frisch, G. W. Trucks, H. B. Schlegel, G. E. Scuseria, M. A. Robb, J. R. Cheeseman, G. Scalmani, V. Barone, B. Mennucci, G. A. Petersson, H. Nakatsuji, M. Caricato, X. Li, H. P. Hratchian, A. F. Izmaylov, J. Bloino, G. Zheng, J. L. Sonnenberg, M. Hada, M. Ehara, K. Toyota, R. Fukuda, J. Hasegawa, M. Ishida, T. Nakajima, Y. Honda, O. Kitao, H. Nakai, T. Vreven, J. A. Montgomery, Jr., J. E. Peralta, F. Ogliaro, M. Bearpark, J. J. Heyd, E. Brothers, K. N. Kudin, V. N. Staroverov, R. Kobayashi, J. Normand, K. Raghavachari, A. Rendell, J. C. Burant, S. S. Iyengar, J. Tomasi, M. Cossi, N. Rega, M. J. Millam, M. Klene, J. E. Knox, J. B. Cross, V. Bakken, C. Adamo, J. Jaramillo, R. Gomperts, R. E. Stratmann, O. Yazyev, A. J. Austin, R. Cammi, C. Pomelli, J. W. Ochterski, R. L. Martin, K. Morokuma, V. G. Zakrzewski, G. A. Voth, P. Salvador, J. J. Dannenberg, S. Dapprich, A. D. Daniels, Ö. Farkas, J. B. Foresman, J. V. Ortiz, J. Cioslowski and D. J. Fox, Gaussian, Inc., Wallingford, CT, 2009.
45 H.-J. Werner, P. J. Knowles, G. Knizia, F. R. Manby, M. Schütz, P. Celani, T. Korona, R. Lindh, A. Mitrushenkov, G. Rauhut, K. R. Shamasundar, T. B. Adler, R. D. Amos, A. Bernhardsson, A. Berning, D. L. Cooper, M. J. O. Deegan, A. J. Dobbyn, F. Eckert, E. Goll, C. Hampel, A. Hesselmann, G. Hetzer, T. Hrenar, G. Jansen, C. Köppl, Y. Liu, A. W. Lloyd, R. A. Mata, A. J. May, S. J. McNicholas, W. Meyer, M. E. Mura, A. Nicklaß, D. P. O'Neill, P. Palmieri, D. Peng, K. Pflüger, R. Pitzer, M. Reiher, T. Shiozaki, H. Stoll, A. J. Stone, R. Tarroni, T. Thorsteinsson and M. Wang, http://www.molpro.net, 2010.
46 H. Eyring, S. H. Lin and S. M. Lin, *Basic Chemical Kinetics*, 1980.
47 V. V. Kislov, T. L. Nguyen, A. M. Mebel, S. H. Lin and S. C. Smith, *J. Chem. Phys.*, 2004, **120**, 7008–7017.
48 P. J. Robinson and K. A. Holbrook, *Unimolecular Reactions*, 1972.
49 J. Steinfield, J. Francisco and W. Hase, *Chemical Kinetics and Dynamics*, 1982.
50 W. B. Miller, S. A. Safron and D. R. Herschbach, *Discuss. Faraday Soc.*, 1967, **44**, 108–122.
51 R. D. Levine, *Molecular Reaction Dynamics*, Cambridge University Press, UK, 2005.

 This journal is © the Owner Societies 2015